

# Multiphoton interference outperforms pairwise overlaps for distinguishability characterization

S. N. van den Hoven,<sup>1</sup> M. C. Anguita,<sup>1</sup> S. Marzban,<sup>1</sup> and J. J. Renema<sup>1</sup>

<sup>1</sup>*MESA+ Institute for Nanotechnology, University of Twente,  
P. O. box 217, 7500 AE Enschede, The Netherlands*

(Dated: December 5, 2025)

We propose a protocol that characterizes the pairwise overlaps of the internal modes of single photons more efficiently than pairwise Hong-Ou-Mandel characterization experiments. This protocol exploits multiphoton interference. We experimentally implement this protocol to characterize three photons. We show that our implementation of the characterization protocol outperforms the pairwise Hong-Ou-Mandel characterization, even if the Hong-Ou-Mandel characterization would have been performed in a noiseless, perfect experiment. We demonstrate this via the Fisher information matrix.

In the paradigm of linear quantum optics, the interference of many single photons has many promising applications. One prominent example is boson sampling, in which samples are drawn from the distribution of many single photons scattered by an interferometer [1]. Experimental realizations of boson sampling were among the first to claim a quantum advantage demonstration [2, 3]. Another key application is universal fault-tolerant quantum computation (UFTQC). Photonics offers a promising platform for UFTQC, where the creation of entangled resource states as well as projective entangling measurements are realized via interference of multiple photons [4, 5]. These photonic entangling operations also enable the distribution of quantum information over large distances for applications like distributed quantum computing [6]. Leveraging multiphoton interference has also led to major advances in quantum sensing, enabling measurement sensitivities beyond the classical shot-noise limit and driving milestones such as Heisenberg-limited phase estimation with NOON-states [7, 8] and squeezed-light interferometry in large-scale detectors [9, 10].

All applications of interference of many (non-interacting) single photons rely on the particles to be indistinguishable. However, realistic single-photon sources do not adhere to this assumption. Imperfections and inconsistencies in the manufacturing processes of single-photon sources result in the generation of single-photons with slightly different wavefunctions (e.g. spectrum, polarization). This partial distinguishability challenges applications, enabling classical simulation of boson sampling [11, 12], or introducing mixedness while performing entangling operations [13–15].

To determine the quality of the photons, usually a characterization experiment is performed. The state-of-the-art method for the pairwise characterization of two single photons is the Hong-Ou-Mandel (HOM) experiment, in which two single photons enter two input arms of a balanced beamsplitter and the ratio between bunched and anti-bunched events is measured. This ratio is a direct function of the overlap of the wavefunction of the two single photons [16]. However, the pairwise charac-

terization of many single photons can quickly become a time consuming process. This motivates us to search for more effective characterization protocols.

The main observation that let us believe that there is room for improvement is that the HOM-characterization features merely two-photon interference, while often an advantage can be obtained by allowing for multiple photons to interfere. Examples include near-deterministic teleportation [17, 18], photonic fusion [19, 20], photon distillation [13, 21–25] and quantum sensing [7–10].

In this work, we investigate whether multiphoton interference can enable characterization protocols that outperform standard HOM-based approaches. Specifically, we consider the following scenario: given access to multiple continuous streams of partially distinguishable single photons and a fully tunable interferometer, can one design a protocol that characterizes all pairwise photon overlaps more efficiently than performing pairwise HOM experiments? We quantify efficiency using the Fisher information matrix (FIM).

We find a protocol that outperforms HOM-characterization for the 3-photon case via numerical optimization. After inspection, we find a circuit that outperforms parallel HOM experiments for the arbitrary  $n$ -photon case.

We experimentally implement the protocol for the 3-photon case and find that the FIM, inferred from experimental data, surpasses what would be achievable in a noiseless experiment using the HOM-characterization protocol. This demonstrates both the practical viability of our approach and the advantage of multiphoton interference for photon characterization.

*Improved characterization for three photons.*—In a boson-sampling-type multiphoton interference experiment with partially distinguishable photons, the probability mass function (pmf) sampled by Fock-basis detection in output configuration  $s$  is given by [26, 27]:

$$P(s) = \frac{1}{\prod_i r_i! s_i!} \sum_{\sigma \in S_n} \left[ \prod_{j=1}^n \mathcal{S}_{j, \sigma(j)} \right] \text{perm}(M \circ M_\sigma^*), \quad (1)$$

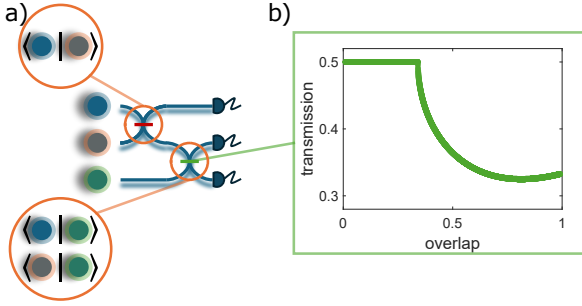


Figure 1. Improved characterization protocol. (a) The linear optical circuit consists of a balanced beamsplitter (indicated as a red horizontal stripe), followed by a beamsplitter with a splitting ratio that is dependent on the quality of the photons. The balanced beamsplitter effectively performs a HOM-characterization, in which information is gained about the pairwise overlap of the uppermost two photons. The second beamsplitter is then used to gain additional information about the pairwise overlaps. (b) The relation between the splitting ratio of the second beamsplitter and the quality of the photons.

where  $M$  is a submatrix of the unitary representation of the interferometer  $U$ , constructed by selecting rows and columns of  $U$  corresponding to the input modes and output modes of interest ( $M = U_{d(\mathbf{r}),d(\mathbf{s})}$ ). Here  $d(\mathbf{r})$  and  $d(\mathbf{s})$  represent the mode assignment lists of the input and output states respectively.  $r_i$  and  $s_i$  denote the  $i^{th}$  element of the mode occupation lists of the input and output states respectively.  $S_n$  denotes the symmetric group,  $S$  denotes the distinguishability matrix where  $S_{i,j} = \langle \psi_i | \psi_j \rangle$  denotes the overlap between photon  $i$  and  $j$  represented by their internal wave functions  $\psi_i$  and  $\psi_j$  respectively.  $\circ$  represents the Hadamard product,  $*$  denotes the element-wise conjugation and  $M_\sigma$  denotes  $M$  where its rows are permuted according to  $\sigma$ . Lastly, the permanent of matrix  $M$  with shape  $n \times n$  is defined as

$$\text{perm}(M) = \sum_{\sigma \in S_n} \prod_{i=1}^n M_{i,\sigma(i)}. \quad (2)$$

For a given input configuration, the pmf in Eq. (1) is a function of the scattering matrix  $U$ , and the distinguishability matrix  $S$ . We assume that  $S$  is defined by unknown parameters we aim to characterize, while the matrix  $U$  is defined by known parameters under our complete control. To estimate this pmf, we draw samples from the corresponding distribution. From the estimated pmf, we then infer the underlying parameters of interest.

However, not all pmfs are equally effective for parameter estimation. The Fisher information matrix provides a rigorous measure of how much information an observable random variable carries about an unknown parameter, with higher values (in the matrix sense) indicating greater sensitivity and, thus, better estimation potential. The Fisher information matrix for a characterization of

three single photons is defined as:

$$[\mathcal{I}(\theta)]_{ij} = \sum_s \left[ \left( -\frac{\partial^2}{\partial \theta_i \partial \theta_j} \log P(s) \right) |\theta \right] P(s), \quad (3)$$

where  $\theta = (|\langle \psi_1 | \psi_2 \rangle|, |\langle \psi_1 | \psi_3 \rangle|, |\langle \psi_2 | \psi_3 \rangle|)$ . Note that we are not including the triad phase [28, 29] as an unknown parameter that needs to be estimated. The reason for this is twofold. First, experiments have been shown to be accurately modeled using models that exclude triad phases [30, 31] and it has been shown that changing the triad phase to a nonzero value often requires considerable effort [28]. Second, our main goal is to find a characterization protocol that outperforms the conventional HOM-characterization protocol. Using the HOM-effect, no information can be obtained about the triad phase, due to the fact that only two photons interfere in a HOM-experiment. We therefore leave out the triad phase in our analysis. However, we point out that another benefit of characterization experiments involving multiphoton interference is the potential to gain information about the triad phases.

We make use of the additive property of the FIM, which allows us to analyze the total information gained across multiple experiments. This means we can consider a collection of different experiments and sum their respective contributions to the FIM. In our approach, we choose to allow for three distinct experimental configurations. This choice is motivated by the fact that the HOM-characterization of three photons, we aim to outperform, also relies on performing three separate experiments.

Each of the three interference experiments can be described by a distinct scattering matrix, where the  $ij^{th}$  element describes the probability amplitude of the transition of a single photon from the input mode  $i$  to the output mode  $j$ . For a lossless passive linear optical system acting on  $N$  modes, this scattering matrix must be unitary and can be uniquely specified by  $2N$  real parameters. Two popular methods to parametrize a linear optical scattering matrix is via the Reck or Clements decompositions [32, 33], in which about half of the real parameters describe the splitting ratios of two-mode beamsplitters and the other half describe the values assigned to phase shifters at various locations. However, in a boson sampling-like experiment, we perform a projective measurement in the Fock-basis after the scattering matrix. This measurement is insensitive to phase information. Of these  $N^2$  parameters, there are exactly  $2N - 1$  parameters that leave the pmf invariant. As a result, we require  $N^2 - (2N - 1) = (N - 1)^2$  parameters to describe a family of scattering matrices that yield the same pmf. We will focus on  $3 \times 3$  matrices that are described by the splitting ratios of three two-mode beamsplitters and one phase shifter.

We used conventional numerical optimization techniques to find 12 parameters that maximize the determinant of the sum of the FIMs corresponding to three dif-

ferent interferometers. We optimize for the determinant of the sum of the FIMs, which corresponds to optimizing for the D-optimality of our experimental design [34]. D-optimality minimizes the volume of uncertainty and is invariant under reparameterization. In general, the optimal experimental design depends on the true values of the unknown parameters. We therefore perform the optimization for different underlying values. We assume we have no prior knowledge about the quality of the photons and therefore we optimize for the situation that the pairwise overlaps are equal. However, if information about a bias in the quality of the photons is available, it can be accounted for by weighting the time allocated to each experiment accordingly.

The results of our numerical optimization are summarized in Fig. (1). Subject to the constraints outlined above, we find that the optimal strategy is to perform three instances of the same experiment, each differing by a permutation of the input configuration of the photons. Additionally, we find that the optimal strategy starts with sending two photons to a balanced beamsplitter, after which a third photon interferes with the state that comes out of one of the output arms of the balanced beamsplitter. The splitting ratio of this second beamsplitter is a function of the (unknown) quality of the photons, the relationship can be found in Fig. (1b).

To better understand the behavior of Fig. (1b), we focus on the state immediately after the balanced beamsplitter, which consists of a bunched and an anti-bunched component. Their relative amplitudes depend on photon indistinguishability, with complete bunching in the completely indistinguishable case. In the regime of high-quality photons, the behavior of the optimal splitting ratio is dominated by the bunched component. This results in an optimal splitting ratio of  $\frac{1}{3}$  in the limit of indistinguishable photons. Noteworthy, this splitting ratio, in combination with a bunched component ( $|021\rangle$ ) results in the  $|012\rangle$  output state being suppressed as a result of destructive quantum interference. In the regime of low-quality photons, the behavior of the optimal splitting ratio is dominated by the anti-bunched component. This results in an optimal splitting ratio of  $\frac{1}{2}$  just like in the HOM-characterization.

*Generalization.*-We point out the resemblance of the protocol in Fig. (1) with the HOM-characterization. This similarity allows us to generalize the scheme to arbitrary numbers of photons outperforming HOM, but without a guarantee of optimality. We note that all information about the interference involving the first beamsplitter can be obtained by measuring the state in one of the two output modes. We thus have the possibility to let the state at the other output arm interfere with the third photon, yielding additional information about pairwise overlaps. This way, we always get more information about pairwise overlaps than we would get in a HOM-characterization. We use this observation to

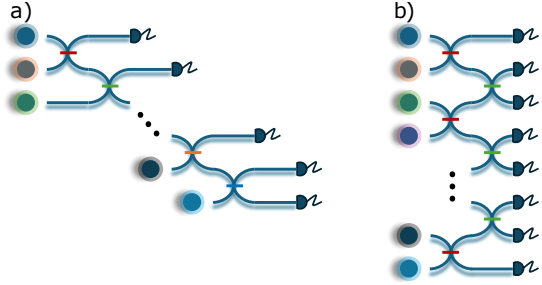


Figure 2. Generalization of multiphoton characterization experiments that will outperform HOM-characterization. (a) A cascade of beamsplitters, each new beamsplitter is attached to the output arm of the previous beam splitter and to a 'fresh' photon. We expect the splitting ratios of the beamsplitters in the cascade to match values such that forbidden outcomes are a result of destructive quantum interference for the dominant contribution to the output state of the previous beamsplitter. (b) Balanced beamsplitters in the first layer perform many HOM-characterization experiments in parallel. The second layer is used to perform additional interference experiments to extract additional information about the pairwise overlaps. We leave the output mode of at least one balanced beamsplitter untouched (the upper one in our schematic) to determine whether a bunching or anti-bunching event occurred at each beamsplitter in the first layer.

propose generalizations of our characterization protocol. Two examples of such generalizations are displayed in Fig. (2). It follows from the considerations presented above that both characterization protocols will outperform the HOM-characterization for any choice of splitting ratios (besides the beamsplitters in the first column, that always need to be balanced).

*Experiment.*-A schematic of the experimental setup, which implements the characterization of three single photons by collecting samples from their distribution after multiphoton interference, is shown in Fig. (3). We generate single photons via degenerate type-II spontaneous parametric down-conversion, featuring a pair of 2mm periodically poled potassium titanyl phosphate (ppKTP) crystals. We down-convert laser light from a pulsed titanium-sapphire laser ( $\Delta\tau \approx 100$  fs), with a central wavelength of 775nm and a FWHM of  $\Delta\lambda = 5.6$ nm. The resulting two-mode squeezed vacuum (TMSV) states are sent through spectral band-pass filters of  $\Delta\lambda = 12$ nm to enhance the purity after heralding. For one TMSV state we herald one of the modes with a superconducting nanowire single-photon detector (SNSPD) to leave a single photon (with high probability) in the resulting mode, which is sent to the integrated, tunable 12-mode interferometer. The other TMSV state is sent directly to the interferometer. We post-select on detecting three photons, projecting the TMSV onto the  $|11\rangle$  state with high probability. By lowering the pump power of the laser, we increase the probability of project-

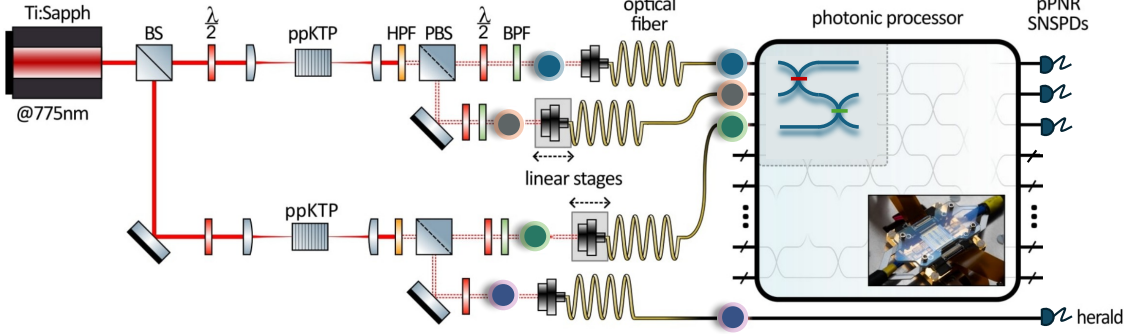


Figure 3. Experimental setup. A Ti:Sapph laser pumps two single-photon sources in parallel. The beam is focused onto a ppKTP crystal to produce pairs of single photons (red wave-packets) via type-II SPDC, then filtered with a high-pass filter (HPF). The two photons are split at a polarizing beam splitter (PBS), filtered with bandpass filters (BPF), and coupled into optical fibers. Linear stages control the path lengths and thus the relative delays of the photons, to optimize temporal overlap of the photons. The first three photons are sent to the photonic chip for the experiments, while the fourth is used as a herald. The scattering matrix presented in Fig. (1) is programmed in the top-left corner of the chip. A picture of the photonic chip is included as an inset. The output state is detected using a bank of quasi-photon-number-resolving superconducting nanowire single-photon detectors (qPNR SNSPDs).

ing onto the desired  $|11\rangle$  state.

The photonic processor consists of a mesh of tunable Mach-Zehnder interferometers (MZIs), integrated in low-loss silicon nitride [35, 36]. The mesh has a configuration following Clements et al. [33]. Tunability is realized via the thermo-optic effect and Joule heating. Using a carefully chosen subset of the available MZIs and feedback, we implement the  $3 \times 3$  scattering matrix as presented in Fig. (1a) with an amplitude fidelity ( $2\sigma$  confidence interval) of  $F = \frac{1}{N} \text{Tr}(|U_{\text{target}}^\dagger||U_{\text{set}}|) = 1 - 0.000022^{+0.000016}_{-0.000074}$ . All three matrices that we need for our characterization are equal up to permutations, so instead of programming three different matrices, we can permute the input modes by manually switching fibers.

The photonic processor is followed by a set of 9 SNSPDs, which are used to create three quasi-photon-number-resolving (qPNR) [37] detectors. The qPNRs are calibrated with a heralded single-photon experiment, and the translation between three-fold coincidence counts to samples of output states is adjusted accordingly.

The measured samples for the three different experiments, with the three different configurations of the input fibers, are used in a maximum likelihood estimate (MLE) for the parameter set  $\theta = (|\langle\psi_1|\psi_2\rangle|, |\langle\psi_1|\psi_3\rangle|, \langle\psi_2|\psi_3\rangle, \phi_{\text{triad}}, t_1, t_2, t_3, \alpha)$ . Here,  $t_1$ ,  $t_2$  and  $t_3$  represent the splitting ratios of the two-mode beam splitters in a 3-mode Clements (or Reck) decomposition,  $\alpha$  describes the phase shifter in this decomposition. Although we do three separate experiments, we assume that the samples are drawn from pmfs that are parametrized by the same set. We used the same interferometer for all experiments, and the interferometer is stable over time. Fig. (4a) shows the measured (and normalized) counts as well as a pmf resulting from the MLE for one of the three experiments.

To avoid cherry picking, we display the pmf with the largest total variational distance (tvd) between model and experiment. The featured pmf has a tvd of 0.041, the other two pmfs can be found in the supplementary material with tvds of 0.024 and 0.020.

Fig. (4b) compares the determinants of the inverses of three FIMs as a function of the number of chronologically obtained samples. The first FIM is computed from our experimental data using Eq. (3). The second FIM represents a perfect HOM-characterization experiment (noiseless, with a perfectly balanced beam splitter). The third FIM represents a perfect implementation of our improved characterization protocol and is included to illustrate the effect of experimental noise. The results clearly indicate that, for the same number of samples, our protocol provides better characterization of pairwise overlaps than a perfect HOM-based approach. Moreover, the observed FIM is only slightly less informative than the ideal FIM for the estimated parameters, demonstrating the robustness of our method in the presence of noise.

*Discussion and conclusion.*—We have shown a novel protocol for the characterization of pairwise overlaps of single photons. This protocol outperforms the conventional and broadly used HOM-characterization protocol, quantified in terms of the Fisher information matrix. This protocol can be understood as an extension of the HOM-characterization and can be used for the characterization of any number of photons. For the case of three photons, we show that our protocol is optimal, it would be interesting to further investigate characterization protocols that feature multiphoton interference for the characterization of  $n$  photons to see if different protocols emerge as optimal.

We experimentally implement this protocol for three photons and demonstrate a favorable observed informa-

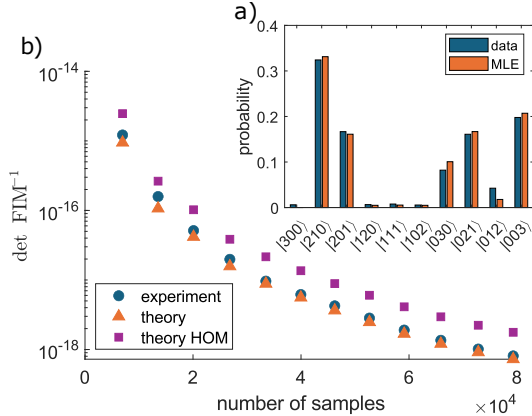


Figure 4. Experimental results. (a) The probability mass function corresponding to the scattering matrix of Fig. (1a), experimentally measured (blue) and modeled (red). (b) The determinant of the inverse of the observed Fisher information matrix is plot against the number of samples (blue circles). The value is compared with the fisher information corresponding to a perfectly executed noiseless HOM-characterization experiment (purple squares) and with a perfectly executed noiseless experiment of our improved characterization protocol (orange triangles). We see that the our experiment consistently outperforms the HOM-characterization.

tion matrix compared to the FIM one would observe if one performed a series of perfect, i.e. noiseless HOM-characterization experiments.

However, we note that it might seem unfair to compare a two-photon experiment with an  $n$ -photon experiment. Typically, the rates at which one can perform a two-photon experiment are much higher than the rates at which one can perform an  $n$ -photon experiment. Fortunately, the interferometer in our proposed characterization protocol can also be used to perform a HOM-experiment by constructing a cumulative pmf. We il-

lustrate this for the case where  $n = 3$  for clarity, but this generalizes to larger photon numbers. This involves collecting samples corresponding to bunching and anti-bunching events. In the scenario where the single-photon sources are heralded, this allows for a characterization experiment that consistently outperforms the HOM-characterization experiment: Attempt to perform the three photon-experiment as presented in this letter, but do not just post-select on 3-photon events. Additionally, whenever the heralded single-photon sources indicate that the upper two sources fired, post select on 2-photon events. This way, at the rates of a 2-photon experiment we characterize the pairwise overlap via a HOM-experiment, and every once in a while we get lucky and perform a 3-photon experiment, with which we get additional information about the overlaps.

Additionally, we would like to mention that the characterization protocol as proposed in this Letter is technologically more demanding, it requires a more complex interferometer and significantly more detectors. However we argue that, the interferometer is actually not much more complex, simply adding beamsplitter(s) after the balanced beamsplitter(s) that is (are) needed for the HOM-characterization suffices. A limited access to detectors could be a reason to stick with a HOM-characterization protocol, which can be implemented already using as little as 4 detectors to measure the full pmf with qPNRDs or even with just two detectors by sacrificing half of the samples.

*Acknowledgments.*-We thank F.H.B. Somhorst, N. Walk and C. Toebe for scientific discussions. This research is supported by the PhotonDelta National Growth Fund program. This publication is part of the project At the Quantum Edge (VI. Vidi.223.075) of the research programme VIDI which is financed by the Dutch Research Council (NWO).

*Data availability.*-All experimental and simulated data used in this study are available in the 4TU.ResearchData database. [38]

---

[1] S. Aaronson and A. Arkhipov, in *Proceedings of the Forty-Third Annual ACM Symposium on Theory of Computing* (Association for Computing Machinery, New York, NY, USA, 2011), STOC '11, p. 333–342, ISBN 9781450306911.

[2] H.-S. Zhong, H. Wang, Y.-H. Deng, M.-C. Chen, L.-C. Peng, Y.-H. Luo, J. Qin, D. Wu, X. Ding, Y. Hu, et al., *Science* **370**, 1460 (2020).

[3] H. Wang, J. Qin, X. Ding, M.-C. Chen, S. Chen, X. You, Y.-M. He, X. Jiang, L. You, Z. Wang, et al., *Phys. Rev. Lett.* **123**, 250503 (2019).

[4] S. Bartolucci, P. Birchall, H. Bombín, H. Cable, C. Dawson, M. Gimeno-Segovia, E. Johnston, K. Kieling, N. Nickerson, M. Pant, et al., *Nat. Commun.* **14**, 912 (2023).

[5] H. Bombín, C. Dawson, R. V. Mishmash, N. Nickerson, F. Pastawski, and S. Roberts, *PRX Quantum* **4**, 020303 (2023), URL <https://link.aps.org/doi/10.1103/PRXQuantum.4.020303>.

[6] D. Barral, F. J. Cardama, G. Díaz-Camacho, D. Faifde, I. F. Llovo, M. Mussa-Juane, J. Vázquez-Pérez, J. Villasuso, C. Piñeiro, N. Costas, et al., *Computer Science Review* **57**, 100747 (2025), ISSN 1574-0137, URL <https://www.sciencedirect.com/science/article/pii/S1574013725000231>.

[7] B. C. Sanders and G. J. Milburn, *Phys. Rev. Lett.* **75**, 2944 (1995), URL <https://link.aps.org/doi/10.1103/PhysRevLett.75.2944>.

[8] T. Nagata, R. Okamoto, J. L. O'Brien, K. Sasaki, and S. Takeuchi, *Science* **316**, 726 (2007),

https://www.science.org/doi/pdf/10.1126/science.1138007, URL <https://www.science.org/doi/abs/10.1126/science.1138007>.

[9] C. M. Caves, Phys. Rev. Lett. **45**, 75 (1980), URL <https://link.aps.org/doi/10.1103/PhysRevLett.45.75>.

[10] J. Aasi, J. Abadie, B. Abbott, R. Abbott, T. Abbott, M. Abernathy, C. Adams, T. Adams, P. Addesso, R. Adhikari, et al., Nature Photonics **7**, 613 (2013).

[11] J. J. Renema, A. Menssen, W. R. Clements, G. Triginer, W. S. Kolthammer, and I. A. Walmsley, Phys. Rev. Lett. **120**, 220502 (2018).

[12] S. N. van den Hoven, E. Kanis, and J. J. Renema, Phys. Rev. A **111**, 052448 (2025), URL <https://link.aps.org/doi/10.1103/PhysRevA.111.052448>.

[13] C. Sparrow, Ph.D. thesis, Imperial College London (2018).

[14] J. Saied, J. Marshall, N. Anand, S. Grabbe, and E. G. Rieffel, *Advancing quantum networking: Some tools and protocols for ideal and noisy photonic systems* (2024), 2403.02515.

[15] P. P. Rohde and T. C. Ralph, Phys. Rev. A **73**, 062312 (2006), URL <https://link.aps.org/doi/10.1103/PhysRevA.73.062312>.

[16] C.-K. Hong, Z.-Y. Ou, and L. Mandel, Phys. Rev. Lett. **59**, 2044 (1987).

[17] E. Knill, R. Laflamme, and G. J. Milburn, nature **409**, 46 (2001).

[18] J. D. Franson, M. M. Donegan, M. J. Fitch, B. C. Jacobs, and T. B. Pittman, Phys. Rev. Lett. **89**, 137901 (2002), URL <https://link.aps.org/doi/10.1103/PhysRevLett.89.137901>.

[19] F. Ewert and P. van Loock, Phys. Rev. Lett. **113**, 140403 (2014), URL <https://link.aps.org/doi/10.1103/PhysRevLett.113.140403>.

[20] W. P. Grice, Phys. Rev. A **84**, 042331 (2011), URL <https://link.aps.org/doi/10.1103/PhysRevA.84.042331>.

[21] J. Marshall, Phys. Rev. Lett. **129**, 213601 (2022).

[22] C. F. D. Faurby, L. Carosini, H. Cao, P. I. Sund, L. M. Hansen, F. Giorgino, A. B. Villadsen, S. N. van den Hoven, P. Lodahl, S. Paesani, et al. (2024), 2403.12866.

[23] F. Hoch, A. Camillini, G. Rodari, E. Caruccio, G. Carvacho, T. Giordani, R. Albiero, N. D. Giano, G. Corrielli, F. Ceccarelli, et al., *Optimal distillation of photonic indistinguishability* (2025), 2509.02296, URL <https://arxiv.org/abs/2509.02296>.

[24] F. H. B. Somhorst, B. K. Sauér, S. N. van den Hoven, and J. J. Renema, *Photon distillation schemes with reduced resource costs based on multiphoton fourier interference* (2024), 2404.14262.

[25] J. Saied, J. Marshall, N. Anand, and E. G. Rieffel, *General protocols for the efficient distillation of indistinguishable photons* (2024), 2404.14217.

[26] M. C. Tichy, Phys. Rev. A **91**, 022316 (2015).

[27] V. Shchesnovich, Phys. Rev. A **91**, 013844 (2015).

[28] A. J. Menssen, A. E. Jones, B. J. Metcalf, M. C. Tichy, S. Barz, W. S. Kolthammer, and I. A. Walmsley, Phys. Rev. Lett. **118**, 153603 (2017), URL <https://link.aps.org/doi/10.1103/PhysRevLett.118.153603>.

[29] V. S. Shchesnovich and M. E. O. Bezerra, Phys. Rev. A **98**, 033805 (2018), URL <https://link.aps.org/doi/10.1103/PhysRevA.98.033805>.

[30] G. Rodari, L. Novo, R. Albiero, A. Suprano, C. T. Tavares, E. Caruccio, F. Hoch, T. Giordani, G. Carvacho, M. Gardina, et al., PRX Quantum **6**, 020340 (2025), URL <https://link.aps.org/doi/10.1103/PRXQuantum.6.020340>.

[31] F. H. Somhorst, R. van der Meer, M. Correa Anguita, R. Schadow, H. J. Snijders, M. de Goede, B. Kassenberg, P. Venderbosch, C. Taballione, J. Epping, et al., Nat. Commun. **14**, 3895 (2023).

[32] M. Reck, A. Zeilinger, H. J. Bernstein, and P. Bertani, Phys. Rev. Lett. **73**, 58 (1994), URL <https://link.aps.org/doi/10.1103/PhysRevLett.73.58>.

[33] W. R. Clements, P. C. Humphreys, B. J. Metcalf, W. S. Kolthammer, and I. A. Walmsley, Optica **3**, 1460 (2016).

[34] K. Smith, Biometrika **12**, 1 (1918), ISSN 00063444, 14643510, URL <http://www.jstor.org/stable/2331929>.

[35] C. G. H. Roeloffzen, M. Hoekman, E. J. Klein, L. S. Wevers, R. B. Timens, D. Marchenko, D. Geskus, R. Dekker, A. Alippi, R. Grootjans, et al., EEE J. Sel. Top. Quant. Elec., 24(4):1–21 (2018).

[36] C. Taballione, R. van der Meer, H. J. Snijders, P. Hooijjschuur, J. P. Epping, M. de Goede, B. Kassenberg, P. Venderbosch, C. Toebe, H. van den Vlekkt, et al., Materials for Quantum Technology **1**, 035002 (2021).

[37] A. Feito, J. S. Lundein, H. Coldenstrodt-Ronge, J. Eisert, M. B. Plenio, and I. A. Walmsley, New Journal of Physics **11**, 093038 (2009), URL <https://dx.doi.org/10.1088/1367-2630/11/9/093038>.

[38] S. van den Hoven, M. Correa Anguita, S. Marzban, and J. Renema, *Data underlying the publication: "multiphoton interference outperforms pairwise overlaps for distinguishability characterization"*, <https://doi.org/10.4121/aea16cd4-1a57-442d-b06c-643fcdb6393.v1> (2025).